Large spatial variations in diffusive CH4 fluxes from a subtropical coastal reservoir affected by sewage discharge in southeast China

Article

Accepted Version

Large Spatial Variations in Diffusive CH_4 Fluxes from a Subtropical Coastal Reservoir Affected by Sewage Discharge in Southeast China

Ping Yang, Hong Yang, Jordi Sardans, Chuan Tong,* Guanghui Zhao, Josep Peñuelas,* Ling Li, Yifei Zhang, Lishan Tan, Kwok Pan Chun, and Derrick Y. F. Lai*

- **Authors**
  - **Ping Yang** - *Key Laboratory of Humid Subtropical Eco-geographical Process of Ministry of Education, Fujian Normal University, Fuzhou 350007, China*; *School of Geographical Sciences, Fujian Normal University, Fuzhou 350007, China*; http://orcid.org/0000-0002-5212-6065
  - **Hong Yang** - *College of Environmental Science and Engineering, Fujian Normal University, Fuzhou 350007, China*; *Collaborative Innovation Center of Atmospheric Environment and Equipment Technology, Jiangsu Key Laboratory of Atmospheric Environment Monitoring and Pollution Control (AEMPC), School of Environmental Science and Engineering, Nanjing University of Information Science and Technology, Nanjing 210044, China*; *Department of Geography and Environmental Science, University of Reading, Reading RG6 6AB U.K.*
  - **Jordi Sardans** - *CSIC, Global Ecology Unit CREAF-CSIC-UAB, Bellaterra, Catalonia 08193, Spain*; *CREAF, Cerdanyola del Vallès, Catalonia 08193, Spain*
  - **Guanghui Zhao** - *School of Geographical Sciences, Fujian Normal University, Fuzhou 350007, China*
  - **Ling Li** - *School of Geographical Sciences, Fujian Normal University, Fuzhou 350007, China*
  - **Yifei Zhang** - *School of Geographical Sciences, Fujian Normal University, Fuzhou 350007, China*
  - **Lishan Tan** - *School of Geographical Sciences, East China Normal University, Shanghai 200241, China*
  - **Kwok Pan Chun** - *Department of Geography, Hong Kong Baptist University, Hong Kong, China*; http://orcid.org/0000-0001-9873-6240

- **Corresponding Authors**
  - **Chuan Tong** - *Key Laboratory of Humid Subtropical Eco-geographical Process of Ministry of Education, Fujian Normal University, Fuzhou 350007, China*; *School of Geographical Sciences, Fujian Normal University, Fuzhou 350007, China*; Email: tongch@fjnu.edu.cn
  - **Josep Peñuelas** - *CSIC, Global Ecology Unit CREAF-CSIC-UAB, Bellaterra, Catalonia 08193, Spain*; *CREAF, Cerdanyola del Vallès, Catalonia 08193, Spain*; Email: Josep.Penuelas@uab.cat
  - **Derrick Y. F. Lai** - *Department of Geography and Resource Management, The Chinese University of Hong Kong, Hong Kong, China*; Email: dyflai@cuhk.edu.hk

ABSTRACT:
Coastal reservoirs are potentially CH_4 emission hotspots owing to their biogeochemical role as the sinks of anthropogenic carbon and nutrients. Yet, the fine-scale spatial variations in CH_4 concentrations and fluxes in coastal reservoirs remain poorly understood, hampering an accurate determination of reservoir CH_4 budgets. In this study, we examined the spatial variability of diffusive CH_4 fluxes and their drivers at a subtropical coastal reservoir in southeast China using high spatial resolution measurements of dissolved CH_4 concentrations and physicochemical properties of the surface water. Overall, this reservoir acted as a consistent source of atmospheric CH_4, with a mean diffusive flux of 16.1 μmol m^{-2} h^{-1}. The diffusive CH_4 flux at the reservoir demonstrated considerable spatial variations, with the coefficients of variation ranging between 199 and 426% over the three seasons. The shallow water zone (comprising 23% of the reservoir area) had a disproportionately high contribution (56%) to the whole-reservoir diffusive CH_4 emissions. Moreover, the mean CH_4 flux in the sewage-affected sectors was significantly higher than that in the nonsewage-affected sectors. The results of bootstrap analysis further showed that increasing the sample size from 10 to 100 significantly reduced the relative standard deviation of mean diffusive CH_4 flux from 73.7 to 3.4%. Our findings highlighted the role of sewage in governing the spatial variations in reservoir CH_4 emissions and the importance of high spatial resolution data to improve the reliability of flux estimates for assessing the contribution of reservoirs to the regional and global CH_4 budgets.

Introduction

Atmospheric greenhouse gas (GHG) concentrations have increased markedly since Industrial Revolution as a result of the ever-increasing anthropogenic GHG emissions.(1,2) Methane (CH_4) is one of the major potent atmospheric GHGs, being 34 times more efficient in trapping heat than carbon dioxide (CO_2) on a per unit mass basis over a 100 year time horizon.(2) In 2018, the global mean atmospheric CH_4 concentration reached a record level of 1869 ppb, exceeding the preindustrial levels by about 150%.(3) Thus, quantifying the strength of CH_4 emissions from various ecosystems has become a top priority in evaluating global climate change and its associated effects on the environment and human society.

Reservoirs are widely distributed in different parts of the world and represent an important component of surface water ecosystems. They receive large amounts of organic matter and nutrients from the catchments, with a considerable fraction being subsequently returned to the atmosphere as GHGs (e.g., CO_2, CH_4, and N_2O). Concerns about CH_4 emissions from reservoirs have increased in recent decades,(4−9) with the suggestion that reservoirs serve as a globally significant source of atmospheric CH_4.(10−13) Hydropower reservoirs around the world are estimated to release about 9.7 Tg CH_4 yr^{-1},(10,14) while a synthesis study showed that total CH_4 emission from global reservoirs amounted to 13.3 Tg yr^{-1}, which was equivalent to approximately 20% of the global inland water CH_4 budget.(12) Meanwhile, a paucity of the CH_4 flux data from reservoirs with varying degrees of human perturbations over a broad range of geographic regions has limited our confidence in constructing reliable reservoir CH_4 budgets.

In continuously flooded reservoirs, microbial CH_4 production is supported by the steady supply of carbon substrates arising from the input of allochthonous organic matter and pelagic primary production,(15−17) as well as the presence of a strongly anoxic environment.(18) Previous studies showed that CH_4 emissions increased initially following the establishment of reservoirs and large dams owing to the decomposition of a large amount of vegetation and organic soil accumulated at the bottom of the reservoir.(19) Yet,

CH_4 emissions would subsequently diminish over time owing to the exhaustion of mineralizable organic matter.(10) At the later stage, allochthonous materials from the watershed become increasingly important as a sustainable source of biogenic substrates for reservoir CH_4 production.(9,17,20−21) Although extremely high levels of CH_4 emissions have been reported from some highly polluted inland freshwater reservoirs, particularly those in close proximity to wastewater discharge sites and influenced by high levels of human activities,(7,9,20,22) these studies were based on field measurements from a limited number of sites without a good spatial coverage across the entire reservoir. Moreover, because these studies were conducted at inland reservoirs only, the magnitude of CH_4 emissions from coastal reservoirs remains a critical gap in the estimation of global reservoir CH_4 budgets. As coastal reservoirs often experience a higher salinity than inland ones, CH_4 production and emission rates might differ between the reservoirs in these two zones.

Continual increase in population size coupled with rapid economic growth and urbanization in the coastal zones have caused drastic changes in the trophic status of coastal aquatic ecosystems, especially in developing countries.(23,24) Anthropogenic wastewater inputs have been shown to substantially increase CH_4 emissions from coastal estuaries, embayments, and lagoons.(1,25−27) Coastal reservoirs are characterized by complex interactions between the terrestrial and marine processes and may act as biogeochemical sinks of terrestrial pollutants. While it is possible that coastal reservoirs are significant CH_4 sources owing to the high inputs of anthropogenic carbon and nutrients, there is currently a lack of empirical data to test this hypothesis and advance our understanding of CH_4 cycling in the coastal zone.

To fill these knowledge gaps, we conducted high spatial resolution measurements of dissolved CH_4 concentrations in a subtropical coastal reservoir in southeast China over three seasons of a year to estimate the diffusive CH_4 fluxes across the water–atmosphere interface. The specific objectives of this study were to: (1) quantify the magnitude of diffusive CH_4 fluxes from a subtropical coastal reservoir; (2) assess the spatial variability and potential hotspots of reservoir CH_4 emissions; and (3) examine the drivers of the spatial variations in reservoir CH_4 emissions, in particular the role of anthropogenic wastewater inputs.

Materials and Methods

Study Area

This study was carried out at the Wenwusha Reservoir (25°49′36″–25°54′00″ N, 119°35′12″–119°38′11″ E) in Fujian Province situated in the coastal area of southeast China (Figure 1). The area is influenced by a humid subtropical monsoonal climate, with an annual mean air temperature and precipitation of 19.3 °C and 1390 mm, respectively. Approximately 75% of precipitation falls in the wet season between May and September. Wenwusha Reservoir is mainly used for irrigation water diversion and flood mitigation, with the total surface area, total volume, and catchment area being 5.2 km^2, 3.20 × 10^8 m^3, and 275 km^2, respectively.

The reservoir was created by constructing two dams at different times at the Nangyangdong River estuary. We divided the reservoir into two zones according to the time of dam construction, land cover types, and trophic status (Figure 1). The northern reservoir zone (NRZ) was established in 1957, with a surface area of 1.9 km^2 and a total volume of 1.40 × 10^8 m^3. Its catchment comprises of mostly farmlands (including aquaculture) as well as cities and towns with a total area of 277 km^2 (Figure 1). Some small drainage channels are directly connected to the municipal and industrial sewage discharge points that are located at the margins of the NRZ. In contrast, the southern reservoir zone (SRZ) was constructed in 2004

and has a larger surface area (3.3 km^2) and total volume (1.69×10^8 m^3) than NRZ. Approximately 70% of its catchment comprises of agricultural land, such as aquaculture ponds and croplands, while its immediate surroundings are forest and wetland habitats (Figure 1). Water salinity in NRZ (0.4–1.3‰) was lower than that in SRZ (0.4–3.7‰), as a result of dilution by freshwater surface runoff.

Sample Collection

Surface water samples were collected at a depth of 20 cm from 103 sites (NRZ = 56; SRZ = 47) distributed along 21 transects (T1–T11 for NRZ and T12–T21 for SRZ) around the reservoir on three occasions (mid-November 2018, and mid-March, and mid-June 2019) (Figure 1). These sites were distributed in five different sewage loading sectors, namely the industrial effluent loading sector (Sector-I), town sewage loading sector (Sector-T), river input sector (Sector-R), aquaculture sewage loading sector (Sector-A), and nonwastewater loading sector (Sector-N). All the transects were accessed using a small motor vessel. Further details about the sampling transects are presented in Figure 1.

Dissolved CH_4 Concentration and Physicochemical Properties of Surface Water

Surface water samples for dissolved CH_4 analysis were collected using a gas-tight water sampler and transferred into 55 mL gas-tight glass serum bottles that were flushed two to three times with the site water thoroughly prior to filling.(28) Then, we injected 0.2 mL of the saturated $HgCl_2$ solution into each sample bottle to kill the microbes(9,29) and immediately sealed the bottle with a butyl rubber stopper without any headspace or bubbles. The samples were stored in an ice box and transported to the laboratory within 6 h. Within 2 d of collection, the dissolved CH_4 concentration of the water samples was determined using the headspace equilibration method.(1,30) Briefly, 25 mL of ultrapure N_2 was injected via a syringe into the glass serum bottle to create a headspace, while 25 mL of the water sample was discarded from the bottle via another syringe that was inserted through the stopper.(31) Then, the bottle was shaken vigorously for 10 min to achieve an equilibrium in the CH_4 concentration between the dissolved and gaseous phases. Subsequently, 5 mL of the headspace air sample was drawn from the bottom using a 5 mL plastic syringe, and injected into a gas chromatograph (GC-2010, Shimadzu, Kyoto, Japan) equipped with a flame ionization detector for CH_4 measurements. The detection limit for the CH_4 concentration was 0.3 ppm, and the relative standard deviation (RSD) of CH_4 analyses was ≤2.0% in 24 h. Dissolved CH_4 concentrations in the water samples were then calculated based on the volumes of water and headspace in the bottle as well as the Bunsen solubility coefficient for CH_4 as a function of temperature and salinity.(32)

For the determination of the concentrations of total organic carbon (TOC), nitrate nitrogen ($N–NO_3^-$), and ammonium nitrogen ($N–NH_4^+$), the surface water sample was collected at each site using a 5 L organic glass hydrophore and transferred into a 150 mL polyethylene bottle. All samples were filtered through a 0.45 μm filter (Biotrans nylon membrane), and the filtrates were stored in 30 mL precombusted glass bottles prior to analysis. The concentration of TOC was measured using a TOC analyzer (TOC-VCPH/CPN, Shimadzu, Japan) with a detection limit of 0.4 μg L^{-1} and a repeatability RSD of ≤1.0% in 24 h. The concentrations of $N–NO_3^-$ and $N–NH_4^+$ were measured with a flow injection analyzer (Skalar Analytical SAN^{++}, The Netherlands), with a detection limit of 0.6 μg L^{-1} and a repeatability RSD of ≤3.0% in 24 h. We also measured various physicochemical parameters of surface water in

situ at a depth of 20 cm at each site. Water temperature (W_T) and pH were determined using a portable pH/mV/temperature meter system (IQ150, IQ Scientific Instruments, USA), while electrical conductivity (EC), salinity, and dissolved oxygen (DO) were measured using an EC meter (2265FS EC, Spectrum Technologies, USA), a salinity meter (Eutech Instruments-Salt6, USA), and a multiparameter water quality checker (HORIBA, Japan), respectively. Air temperature (A_T), atmospheric pressure (A_P), and wind speed (W_S) were measured at 2 m above the water surface using a portable weather meter (Kestrel-3500, USA). Water depths were measured using a portable ultrasonic water depth sensor (GAMICOS, China).

Calculation of Diffusive CH_4 Fluxes

Diffusive CH_4 fluxes (F_D, μg CH_4 m^{-2} h^{-1}) across the water–atmosphere interface were calculated using the thin boundary layer method,(1,8,20,31,33) according to the following equation

$$F_D = k \times (C_{obs} - C_{eq}) \times M \times 1000 \quad (1)$$

where k is the gas transfer velocity (m h^{-1}), C_{obs} is the dissolved CH_4 concentration in surface water (μmol L^{-1}), and C_{eq} is the equilibrium dissolved CH_4 concentration relative to atmospheric concentration at in situ temperature and salinity (μmol L^{-1}), and M is the molar mass of CH_4 (16 g mol^{-1}).

The gas transfer velocity of lentic systems (e.g., lakes, reservoirs, and ponds) is mainly governed by wind speed because of negligible surface water flow.(34) In this study, the k value was calculated using the relationship with wind speed formulated by Cole and Caraco (1998)(35)

$$k = (Sc/600)^{-0.5} \times (2.07 + 0.215 \times U_{10}^{1.7}) \quad (2)$$

where Sc is the Schmidt number for CH_4 calculated as a function of water temperature (see Wanninkhof, 1992),(36) and U_{10} is the frictionless wind speed at 10 m above the water surface (m s^{-1}), which is calculated using(8,37)

$$U_{10} = U_z\left[1 + \frac{(C_{d10})^{1/2}}{K}\ln\left(\frac{10}{z}\right)\right] \quad (3)$$

where U_z (m s^{-1}) is the wind speed at height z (m) above the water surface (2 m in this study), and C_{d10} is the drag coefficient at 10 m above the water surface (0.0013 m s^{-1}), and K is the von Karman constant (0.41).

Statistical Analysis

We applied ANOVA to test for significant ($p < 0.05$) effects of the reservoir zone, sewage sector, and water depth on diffusive CH_4 fluxes and surface water physicochemical properties using Statistica 8.0 (StatSoft, Inc. Tulsa, USA). Principal component analysis (PCA) was used to examine the relationships between water physicochemical parameters and CH_4 concentrations/fluxes using IBM SPSS statistics 22.0 (IBM, Armonk, NY, USA). To examine the influence of sample size on the estimation of whole-reservoir CH_4 emissions, we conducted a bootstrap analysis of seasonal mean CH_4 fluxes by selecting a subset of the 103 sites (n = 10, 20, 30, ..., 100) without replacements and calculating an average value. This process was then repeated 1000 times and the overall mean and standard deviation of CH_4 emissions were calculated for each sample size. More details about the statistical analysis can be found in the Supporting Information.

Results

Effects on Surface Water Physicochemical Properties

Reservoir Zone

Surface water physicochemical properties varied significantly between the two reservoir zones on all three sampling occasions, with higher levels of EC, salinity, and DO and lower concentrations of $N–NO_3^-$ and TOC in SRZ than in NRZ ($p < 0.05$) (Table 1).

Sewage Sector

The mean TOC, $N–NH_4^+$, DO, and salinity differed significantly among the five sewage loading sectors over the three sampling campaigns (Figure 2). Mean TOC and $N–NH_4^+$ concentrations were significantly lower in Sector-N than the other sectors ($p < 0.05$), and were generally highest in Sector-R. In contrast, mean DO concentration was significantly greater in Sector-N than in the other four sectors ($p < 0.05$).

Water Depth

Mean concentrations of TOC and $N–NH_4^+$ varied significantly with water depth ($p < 0.05$), with higher concentrations being observed in the shallow zone (<1 m) than in deeper zones (Figures S1a,b). In contrast, the mean DO concentrations were significantly lower in the shallow zone than in the other two deeper zones across all sampling campaigns ($p < 0.01$; Figure S1c). No significant differences in water salinity were detected among the three depth zones ($p > 0.05$; Figure S1d).

Effects on Surface Water CH_4 Fluxes

Reservoir Zone

Across all sampling sites in the reservoir, diffusive CH_4 fluxes in November 2018, March 2019, and June 2019 ranged from −4.54 to 178, 1.20 to 724, and 0.55 to 578 μmol m^{-2} h^{-1} (Figure 3), respectively, with mean CH_4 emission rates of 13.7 ± 2.68, 16.9 ± 7.08, and 17.7 ± 5.69 μmol m^{-2} h^{-1} in the three sampling campaigns. The mean diffusive CH_4 fluxes were significantly greater in NRZ (21.1 ± 5.65 μmol m^{-2} h^{-1}) than in SRZ (10.1 ± 1.39 μmol m^{-2} h^{-1}) ($p < 0.05$; Figure 4) across the three sampling campaigns.

Sewage Sector

Across the three sampling campaigns, significant differences in mean diffusive CH_4 fluxes were observed among the five sewage loading sectors ($p < 0.01$; Figure 5). Sector-N had significantly lower mean CH_4 fluxes (5.45 ± 0.77, 5.68 ± 0.88, and 7.36 ± 0.57 μmol m^{-2} h^{-1}) than the other four sectors over the whole study period, while Sector-R had significantly higher mean CH_4 fluxes (68.09 ± 27.69, 130.16 ± 99.27, and 96.02 ± 80.43 μmol m^{-2} h^{-1}) than other sectors ($p < 0.05$; Figure 5).

Water Depth

Over the study period, diffusive CH_4 fluxes in depth zones of <1 m, 1–3 m, and >3 m ranged from 23.8 ± 6.16 to 33.3 ± 17.1, 6.79 ± 1.23 to 9.16 ± 0.78, and 4.34 ± 0.57 to 6.12 ± 0.82 μmol m^{-2} h^{-1}, respectively, with mean fluxes of 29.8 ± 3.03, 8.35 ± 0.78, and 4.98 ± 0.57 μmol m^{-2} h^{-1}, respectively (Figure 6). Significantly higher diffusive CH_4 fluxes were observed in the shallow water zone (<1 m deep) than the other two deeper zones (p < 0.05; Figure 6).

Physicochemical Drivers of Variations in CH_4 Fluxes

Over the whole study period, diffusive CH_4 fluxes in the reservoir were positively correlated with air temperature, $N–NH_4^+$, and TOC, and negatively correlated with EC, salinity, and DO (p < 0.05; Table 2). Within each sampling occasion, the spatial variation in diffusive CH_4 fluxes was also positively correlated with that of TOC (r = 0.63–0.79, p < 0.01) and $N–NH_4^+$ (r = 0.23–0.47, p < 0.05), and negatively correlated with that of DO (r = −0.34 to −0.74, p < 0.05) and salinity (r = −0.26 to −0.47, p < 0.01, except June 2019) (Table 2). Surprisingly, air temperature was significantly correlated with CH_4 flux only in November 2018 but not March and June 2019. The results of PCA between the surface water physicochemical properties and CH_4 concentrations and fluxes showed that principal component (PC) I, which represented water quality with positive eigenvectors for $N–NO_3^-$, $N–NH_4^+$, and TOC, explained 78–98% of the variance, while PC II, which reflected water biochemical processes with negative eigenvectors for EC, salinity, and DO, explained another 2–12% of the variance (Figure 7).

Effects on Estimated Whole-Reservoir CH_4 Fluxes

Sample Size

The results of bootstrap analysis showed that the reliability of mean diffusive CH_4 flux across the whole reservoir increased considerably with the number of sampling sites included in flux estimations (Figure 8). The estimated mean diffusive flux varied largely over the 1000 simulations when only 10 samples were selected, with a standard deviation of 12.2 μmol m^{-2} h^{-1} and a RSD of 73.7% (Figure 8b). The simulations produced a large number of flux estimates that were much larger than the average flux of 16.1 μmol m^{-2} h^{-1} obtained from all the 103 sites combined (Figure 8a). Meanwhile, the standard deviation of estimated diffusive flux was shown to decrease continually with sample size to less than 5 μmol m^{-2} h^{-1} and a minimum of 0.6 μmol m^{-2} h^{-1} at a sample size of 40 and 100, respectively (Figure 8b). The RSD of mean diffusive flux was reduced to 3.4% at a sample size of 100, indicating the estimated whole-reservoir CH_4 emissions were less variable and closer to the overall mean.

Spatial Coverage

We upscaled the diffusive CH_4 fluxes obtained from our field measurements to the whole-reservoir scale based on four scenarios of sample site selection, and compared the upscaled fluxes to the best flux estimate (i.e., 0.012 Gg CH_4 yr^{-1}) derived from the spatially averaged flux from all our 103 sites and the total reservoir area (5.2 km^2). Table 3 summarizes the results of total annual diffusive CH_4 fluxes from the reservoir obtained from different scenarios. The first scenario involved the extrapolation of mean flux from a single reservoir zone to the entire reservoir. It was shown that the total CH_4 emissions upscaled from the averages in SRZ and NRZ were 0.007 and 0.016 Gg CH_4 yr^{-1}, respectively, leading to biases in flux estimates by 42 and 33%. In the second scenario, total fluxes were derived from the

mean fluxes in the sewage discharge and nonsewage discharge sectors over the three sampling occasions. Results showed that total CH_4 fluxes were overestimated by 142% based on the data from sewage discharge sectors only (0.029 Gg CH_4 yr^{-1}) but underestimated by 67% based on the data from nonsewage discharge sectors only (0.004 Gg CH_4 yr^{-1}). In the third scenario, the total fluxes were extrapolated from the mean emissions from the shallow (<1 m) or deep water zones alone, leading to an overestimation by 83% (0.022 Gg CH_4 yr^{-1}) and an underestimation by 58% (0.005 Gg CH_4 yr^{-1}), respectively. In the last scenario, the average flux obtained from two different transects was used to estimate the total reservoir CH_4 fluxes. This approach resulted in the greatest bias in estimated whole-reservoir flux, with an underestimation of 83% (0.002 Gg CH_4 yr^{-1}) based on the low mean flux value in Transect 2 but an overestimation of 692% (0.095 Gg CH_4 yr^{-1}) based on the high mean flux in Transect 12.

Discussion

Subtropical Coastal Reservoirs as Net Sources of Atmospheric CH_4

Although CH_4 dynamics in coastal reservoirs were relatively understudied, the magnitude of dissolved CH_4 concentrations found in this study was comparable to those previously reported in the inland reservoirs in the tropical,(4,38) subtropical,(8,9) and temperate(20,22,39) regions (Table 4). The dissolved CH_4 concentrations in our subtropical coastal reservoir were supersaturated with respect to atmospheric equilibrium, indicating that this reservoir acted as a net source of atmospheric CH_4. The magnitude of mean diffusive CH_4 emissions observed in this study (16.1 μmol m^{-2} h^{-1}) was similar to that observed in other tropical,(4,38,40) subtropical,(8,9,41,42) and temperate(20,39,43) reservoirs, but was considerably lower than those reported in the reservoirs in Furnas in Brazil(40) and Harsha in the USA(22) (104–608 μmol m^{-2} h^{-1}; Table 4).

Although the average CH_4 fluxes from our studied reservoir were not particularly high among the world's reservoirs on a per unit area basis, the role of subtropical coastal reservoirs in the regional CH_4 budget should not be overlooked. When the measured fluxes were upscaled to the entire reservoir surface, the total CH_4 emissions from the 5.2 km^2 Wenwusha Reservoir were estimated to be 0.012 Gg CH_4 yr^{-1}. The total diffusive CH_4 flux from coastal reservoirs would account for approximately 1.5% of the annual total from all reservoirs in China.(44) Our findings suggested that CH_4 emissions from coastal reservoirs should be quantified more widely for an accurate assessment of regional and global reservoir CH_4 budgets and an improved estimation of GHG emission inventories.

Role of Sewage Inputs in CH_4 Emissions

Results from our spatially intensive sampling showed that the coastal reservoir represented a consistent source of atmospheric CH_4 that could be intensified by human activities, particularly the inputs of human wastes to water (Figure 3). Considerable small-scale spatial variability of CH_4 emissions has been reported from other inland freshwater reservoirs(4,8,40,45) and lakes(31,46) that could be attributed to the effects of organic matter and nutrient availability. Among the environmental variables recorded in this study, wind speed, water temperature, and atmospheric pressure were relatively constant across the reservoir, while the concentrations of TOC, $N–NO_3^-$, $N–NH_4^+$, and DO showed large spatial

variations (Figure 2). Located in a catchment with intensive human activity, the Wenwusha Reservoir is directly affected by sewage inputs from domestic and industrial effluents, aquaculture pond drainage, as well as river and stormwater runoff (Figure 1). Our results showed that the river input sector had the highest mean TOC and $N–NH_4^+$ concentrations, suggesting the key influence of the upstream area in sustaining the supply of carbon and nitrogen. In addition, the nonwastewater loading sector had significantly lower TOC and $N–NH_4^+$ concentrations and significantly higher DO concentration than all other wastewater loading sectors, indicating a better water quality in the absence of sewage influence. The large spatial variation in nutrient status in the surface water across the reservoir as a result of varying extents of sewage inputs was likely one of the factors influencing CH_4 emissions (Figure 3).

In aquatic ecosystems, CH_4 production is mainly driven by the anaerobic decomposition of organic matter in sediments.(31,47,48) An increase in nutrient loading not only will enhance CH_4 production by stimulating autochthonous production and substrate supply, but also suppress aerobic CH_4 oxidation by intensifying oxygen consumption associated with organic matter degradation.(31,49,50) Although CH_4 production data were not available in this study, our observation of greater CH_4 emissions from the sewage loading sectors than the nonwastewater loading sector lent support to the hypothesis of an enhanced methanogenesis under higher nutrient loads. Our results showed that CH_4 fluxes were positively correlated with TOC and $N–NH_4^+$ concentrations (Table 2), as reported similarly in other aquatic ecosystems,(7,9,51,52) indicating the influence of carbon and nutrient supply on microbial-mediated CH_4 production and emission.

The differences in mean CH_4 fluxes between the two reservoir zones provided additional evidence for the role of sewage drainage in governing CH_4 emissions from this coastal reservoir. Over the study period, mean CH_4 fluxes were consistently found to be greater in NRZ than SRZ (Figures 2 and 4). This could be attributed to the significantly higher $N–NO_3^-$ and TOC concentrations found in NRZ in supporting methanogenic activities (Table 1), as a result of the inflow of nutrient-enriched river runoff and sewage effluents. Previous studies have also demonstrated the positive effect of sewage discharge on CH_4 emissions from streams and a coastal bay.(1,53) At the same time, we observed a significantly lower mean water salinity in NRZ than in SRZ (Table 1) and a significant negative correlation between salinity and CH_4 fluxes over the whole study period (Table 2). Yet, salinity was likely not a dominant factor in governing the spatial variations in CH_4 fluxes in this reservoir because the difference in mean salinity between the two reservoir zones was actually small (<2 ppt) and the spatial heterogeneity of water salinity within each zone was also very low (Table 1). Our findings suggested that salinity would have a limited influence on the spatial variations in CH_4 emissions from coastal reservoirs that do not have direct and open exchange of water with the coastal zone.

We found that the dissolved CH_4 concentrations in the aquaculture ponds, rivers, and municipal sewage drainage channels adjacent to Wenwusha Reservoir were approximately three to eight times higher than those in the reservoir surface water, which could lead to a direct input of dissolved CH_4 into the reservoir and subsequently a steeper CH_4 concentration gradient between the surface water and atmosphere for diffusive emissions. Given a mean river discharge of 54.3 $m^3 s^{-1}$ and a mean dissolved CH_4 concentration of 6.16 μmol L^{-1} in river water over the study period (unpublished data), we estimated that the direct input of

dissolved CH_4 from river runoff into the reservoir was 0.169 Gg CH_4 yr^{-1}, which was over 14 times greater than the annual total amount of CH_4 released from the whole reservoir. Hence, the impacts of river and sewage discharge on the direct introduction of dissolved CH_4 into the reservoir should not be ignored because this external CH_4 addition could well sustain substantial CH_4 emissions from the reservoir surface into the atmosphere even without any internal CH_4 production within the reservoir system. Further studies should be conducted to evaluate the influence of other sewage sources on the direct import of dissolved CH_4 into the reservoir, as well as the relationships between sewage discharge and socioeconomic characteristics of the watershed (e.g., population) to improve our understanding and prediction of reservoir CH_4 dynamics.

Contribution of Shallow Water Zone to Reservoir CH_4 Emissions

We found that diffusive CH_4 fluxes consistently decreased along the hydrologic gradient from the shallow water zone (<1 m) to deeper water zone (>3 m) in the core part of the reservoir (Figures 3 and 6). Previous studies have also reported a negative relationship between CH_4 fluxes and water depth.(8,46,54−57) In the Wenwusha Reservoir, the three hydrologic zones with water depths of <1, 1–3, and >3 m occupied 23, 45, and 32%, respectively, of the total reservoir area. Yet, the area-weighted fluxes from the above three hydrologic zones accounted for 56, 31, and 13%, respectively, of the total reservoir CH_4 emissions, implying that the shallow water zone had a disproportionally large contribution to the overall CH_4 release from this subtropical coastal reservoir.

The shallow water zone near the shore often directly receives sewage discharge, catchment runoff, and river inflows, leading to greater deposition of fresh sediments and organic matter that could potentially increase CH_4 production as compared to the deeper interior zone.(16,31,58) Indeed, greater CH_4 fluxes from the shallow zones have been widely reported in freshwater reservoirs and lakes.(31,46,54,59,60) In this study, the shallow water zone had significantly higher mean TOC (Figure S1a) and $N–NH_4^+$ concentrations (Figure S1b) than the deeper zones, respectively, which corresponded well to the spatial variations in CH_4 fluxes with water depths (Figure 5). Interestingly, we observed high CH_4 emission rates from the unpolluted shallow zones of SRZ, which was possibly related to the continuous inputs of organic matter from nearby wetlands that supported CH_4 production.

The magnitude of net CH_4 release from aquatic systems is determined by methanogenic CH_4 production, methanotrophic CH_4 oxidation, and various CH_4 transport processes. The rate of CH_4 emission from the water surface into the atmosphere can be reduced by CH_4 oxidation,(61) which is partly regulated by the DO level in the water column.(62,63) High rates of CH_4 oxidation have been observed under high concentrations of both dissolved CH_4 and DO.(61−64) It has been suggested that CH_4 oxidation rates are greater in deeper water because of a longer distance for CH_4 transport and thus a higher chance for methanotrophs to take actions.(65) In this study, we found significantly lower mean DO concentrations in the shallow water (<1 m) zone than the two deeper zones (Figure S1c) and a significant and negative correlation between CH_4 fluxes and water DO concentrations (Table 2). These results suggested that high CH_4 emissions from the shallow water zone could also be a result of low rates of CH_4 oxidation arising from the low

O_2 availability and a short CH_4 transport pathway. Further studies in the field and laboratory are needed to test this hypothesis of mechanistic control of net CH_4 fluxes.

Implications of High Spatial Resolution Measurements of CH_4 Fluxes

Our results of flux upscaling to the whole-reservoir scale based on different scenarios of sample site selection showed that the annual flux estimates derived from low spatial resolution measurement in previous studies were subjected to potentially large biases.(8,40,45) We found that the total reservoir CH_4 emissions estimated from the data from single transects were highly unreliable with a bias of up to 692%, probably owing to the low number of sampling sites included in calculating a spatially representative mean flux (Table 3). On the other hand, the estimation of whole-reservoir CH_4 fluxes based on data from the nonwastewater loading sectors only without considering the emission hotspots in the sewage loading sectors could cause a 67% underestimation of total CH_4 emissions (Table 3). Thus, high spatial resolution flux measurements that adequately capture the spatial heterogeneity of the source area are essential for an accurate upscaling of reservoir CH_4 emissions and the development of regional and global reservoir CH_4 budgets.(8,40)

We further evaluated the effect of sample size on the reliability of the estimated mean diffusive CH_4 flux across the whole 5.2 km^2 large reservoir with bootstrap analysis by selecting a subset out of our 103 sites without replacements and repeating this sampling for 1000 simulations. Our results showed that the RSD of mean CH_4 flux decreased continually from 73.7% at a sample size of 10 to 3.4% at a sample size of 100 (Figure 8). Thus, increasing the sample size could effectively reduce the uncertainty and bias of the estimation of whole-reservoir CH_4 emissions. The relationship established between the standard deviation of diffusive CH_4 fluxes and the number of samples as shown in Figure 8 could be used to determine an optimal sample size that could produce a reasonably good flux estimate while keeping the sampling effort to an acceptable level. Similar analysis should be done for reservoirs with varying areas and degrees of human influence for evaluating an appropriate number of sampling sites in quantifying a representative estimate of whole-reservoir CH_4 emissions.

Study Limitations and Recommendations for Future Research

As in most studies, there were some limitations to this study. First, a thorough understanding of the spatial variations in CH_4 concentrations in coastal reservoirs is still lacking, in particular the vertical patterns of dissolved CH_4 along the water column. Future studies should quantify the vertical profile of CH_4 concentrations in the coastal reservoirs in order to improve the estimation of diffusive fluxes. Second, ebullition is often considered an important pathway of CH_4 emissions in reservoirs with high levels of spatial variability.(4,5,45,66) Although previous studies have suggested that shallow water zones are hotspots of CH_4 ebullition in freshwater reservoirs,(4,46,67) we were unable to confirm these patterns owing to the lack of CH_4 ebullition measurements in the Wenwusha Reservoir. Future studies should utilize advanced technologies such as hydroacoustic echosounders to measure CH_4 ebullition directly in coastal reservoirs. Finally, this study did not assess the contribution of individual mechanistic processes, for example CH_4 production and oxidation,

as well as the abundance and activity of various microorganisms, for example methanogens, methanotrophs, and sulfate-reducing bacteria, that are important in CH_4 dynamics. More detailed investigations of the microbial processes involved in CH_4 metabolism can help enhance our understanding of the controls of spatial variations in CH_4 emissions from coastal reservoirs.

Acknowledgments

This research was financially supported by the National Science Foundation of China (nos. 41801070 and 41671088), the National Science Foundation of Fujian Province (no. 2018J01737), Project funded by Fuzhou Cultural Tourism Investment Group Co., Ltd, the Research Grants Council of the Hong Kong Special Administrative Region, China (CUHK458913, 14302014, and 14305515), the CUHK Direct grant (SS15481), the Open Research Fund Program of Jiangsu Key Laboratory of Atmospheric Environment Monitoring and Pollution Control (KHK1806), a project funded by the Priority Academic Program Development of Jiangsu Higher Education Institutions (PAPD), and the Minjiang Scholar Program. JP and JS were supported by the European Research Council grant ERC-SyG-2013-610028 IMBALANCE-P. We would like to thank Miaohui Lu and Chen Tang of the School of Geographical Sciences, Fujian Normal University, for their field assistance.

References

1 Cotovicz, L. C., Jr.; Knoppers, B. A.; Brandini, N.; Poirier, D.; Costa Santos, S. J.; Abril, G. Spatio-temporal variability of methane (CH4) concentrations and diffusive fluxes from a tropical coastal embayment surrounded by a large urban area (Guanabara Bay, Rio de Janeiro, Brazil). Limnol. Oceanogr. 2016, 61, S238– S252, DOI: 10.1002/lno.10298

2 IPCC. Climate Change the Physical Science Basis. Contribution of Working Group I to the Fifth Assessment Report of the Intergovernmental Panel on Climate Change; Stocker, T. F. , Eds; Cambridge University Press: Cambridge, 2013.

3 World Meteorological Organization. WMO Greenhouse Gas Bulletin No. 15; WMO, 2019.

4 DelSontro, T.; Kunz, M. J.; Kempter, T.; Wüest, A.; Wehrli, B.; Senn, D. B. Spatial heterogeneity of methane ebullition in a large tropical reservoir. Environ. Sci. Technol. 2011, 45, 9866– 9873, DOI: 10.1021/es2005545

5 Deshmukh, C.; Guérin, F.; Labat, D.; Pighini, S.; Vongkhamsao, A.; Guédant, P.; Rode, W.; Godon, A.; Chanudet, V.; Descloux, S.; Serça, D. Low methane (CH4) emissions downstream of a monomictic subtropical hydroelectric reservoir (Nam Theun 2, Lao PDR). Biogeosciences 2016, 13, 1919– 1932, DOI: 10.5194/bg-13-1919-2016

6 Guerin, F.; Abril, G.; Serca, D.; Delon, C.; Richard, S.; Delmas, R.; Tremblay, A.; Varfalvy, L. Gas transfer velocities of CO2 and CH4 in a tropical reservoir and its river downstream. J. Mar. Syst. 2007, 66, 161– 172, DOI: 10.1016/j.jmarsys.2006.03.019

7 Martinez-Cruz, K.; Gonzalez-Valencia, R.; Sepulveda-Jauregui, A.; Plascencia-Hernandez, F.; Belmonte-Izquierdo, Y.; Thalasso, F. Methane emission from aquatic ecosystems of Mexico City. Aquat. Sci. 2017, 79, 159– 169, DOI: 10.1007/s00027-016-0487-y

8 Musenze, R. S.; Grinham, A.; Werner, U.; Gale, D.; Sturm, K.; Udy, J.; Yuan, Z. Assessing the spatial and temporal variability of diffusive methane and nitrous oxide emissions from subtropical freshwater reservoirs. Environ. Sci. Technol. 2014, 48, 14499– 14507, DOI: 10.1021/es505324h

9 Wang, X.; He, Y.; Yuan, X.; Chen, H.; Peng, C.; Yue, J.; Zhang, Q.; Diao, Y.; Liu, S. Greenhouse gases concentrations and fluxes from subtropical small reservoirs in relation with watershed urbanization. Atmos. Environ. 2017, 154, 225– 235, DOI: 10.1016/j.atmosenv.2017.01.047

10 Barros, N.; Cole, J. J.; Tranvik, L. J.; Prairie, Y. T.; Bastviken, D.; Huszar, V. L. M.; Del Giorgio, P.; Roland, F. Carbon emission from hydroelectric reservoirs linked to reservoir age and latitude. Nat. Geosci. 2011, 4, 593– 596, DOI: 10.1038/ngeo1211

11 Bastviken, D.; Tranvik, L. J.; Downing, J. A.; Crill, P. M.; Enrich-Prast, A. Freshwater methane emissions offset the continental carbon sink. Science 2011, 331, 50, DOI: 10.1126/science.1196808

12 Deemer, B. R.; Harrison, J. A.; Li, S.; Beaulieu, J. J.; Delsontro, T.; Barros, N.; Bezerra-Neto, J. F.; Powers, S. M.; dos Santos, M. A.; Vonk, J. A. Greenhouse gas emissions from reservoir water surfaces: a new global synthesis. BioScience 2016, 66, 949– 964, DOI: 10.1093/biosci/biw117

13 St Louis, V. L.; Kelly, C. A.; Duchemin, E.; Rudd, J. W. M.; Rosenberg, D. M. Reservoir surfaces as sources of greenhouse gases to the atmosphere: a global estimate. Bioscience 2000, 50, 766– 775, DOI: 10.1641/0006-3568(2000)050[0766:RSASOG]2.0.CO;2

14 Hertwich, E. G. Addressing biogenic greenhouse gas emissions from hydropower in LCA. Environ. Sci. Technol. 2013, 47, 9604– 9611, DOI: 10.1021/es401820p

15 Guérin, F.; Abril, G.; de Junet, A.; Bonnet, M.-P. Anaerobic decomposition of tropical soils and plant material: implication for the CO2 and CH4 budget of the Petit Saut reservoir. Appl. Geochem. 2008, 23, 2272– 2283, DOI: 10.1016/j.apgeochem.2008.04.001

16 Huttunen, J. T.; Vaisanen, T. S.; Hellsten, S. K.; Heikkinen, M.; Nykanen, H.; Jungner, H.; Niskanen, A.; Virtanen, M. O.; Lindqvist, O. V.; Nenonen, O. S.; Martikainen, P. J. Fluxes of CH4, CO2, and N2O in hydroelectric reservoirs Lokka and Porttipahta in the northern boreal zone in Finland. Global Biogeochem. Cycles 2002, 16, 1003, DOI: 10.1029/2000gb001316

17 Maeck, A.; DelSontro, T.; McGinnis, D. F.; Fischer, H.; Flury, S.; Schmidt, M.; Fietzek, P.; Lorke, A. Sediment trapping by dams creates methane emission hot spots. Environ. Sci. Technol. 2013, 47, 8130– 8137, DOI: 10.1021/es4003907

18 Giles, J. Methane quashes green credentials of hydropower. Nature 2006, 444, 524– 525, DOI: 10.1038/444524b

19 Abril, G.; Guerin, F.; Richard, S.; Delmas, R.; Galy-Lacaux, C.; Gosse, P.; Tremblay, A.; Varfalvy, L.; Dos Santos, M. A.; Matvienko, B. Carbon dioxide and methane emissions and the carbon budget of a 10-year old tropical reservoir (Petit Saut, French Guiana). Global Biogeochem. Cycles 2005, 19. DOI: 10.1029/2005gb002457

20 Descloux, S.; Chanudet, V.; Serça, D.; Guérin, F. Methane and nitrous oxide annual emissions from an old eutrophic temperate reservoir. Sci. Total Environ. 2017, 598, 959–972, DOI: 10.1016/j.scitotenv.2017.04.066

21 Vörösmarty, C. J.; Meybeck, M.; Fekete, B.; Sharma, K.; Green, P.; Syvitski, J. P. M. Anthropogenic sediment retention: major global impact from registered river impoundments. Global Planet. Change 2003, 39, 169– 190, DOI: 10.1016/s0921-8181(03)00023-7

22 Beaulieu, J. J.; Smolenski, R. L.; Nietch, C. T.; Townsend-Small, A.; Elovitz, M. S. High methane emissions from a midlatitude reservoir draining an agricultural watershed. Environ. Sci. Technol. 2014, 48, 11100– 11108, DOI: 10.1021/es501871g

23 Lacerda, L. D.; Molisani, M. M.; Sena, D.; Maia, L. P. Estimating the importance of natural and anthropogenic sources on N and P emission to estuaries along the Ceará state coast NE Brazil. Environ. Monit. Assess. 2008, 141, 149– 164, DOI: 10.1007/s10661-007-9884-y

24 Páez-Osuna, F.; Álvarez-Borrego, S.; Ruiz-Fernández, A. C.; García-Hernández, J.; Jara-Marini, M. E.; Bergés-Tiznado, M. E.; Piñón-Gimate, A.; Alonso-Rodríguez, R.; Soto-Jiménez, M. F.; Frías-Espericueta, M. G.; Ruelas-Inzunza, J. R.; Green-Ruiz, C. R.; Osuna-Martínez, C. C.; Sánchez-Cabeza, J.-A. Environmental status of the Gulf of California: a pollution review. Earth-Sci. Rev. 2017, 166, 181– 205, DOI: 10.1016/j.earscirev.2017.01.014

25 Burgos, M.; Sierra, A.; Ortega, T.; Forja, J. M. Anthropogenic effects on greenhouse gas (CH4 and N2O) emissions in the Guadalete River Estuary (SW Spain). Sci. Total Environ. 2015, 503–504, 179– 189, DOI: 10.1016/j.scitotenv.2014.06.038

26 Nirmal Rajkumar, A.; Barnes, J.; Ramesh, R.; Purvaja, R.; Upstill-Goddard, R. C. Methane and nitrous oxide fluxes in the polluted Adyar River and estuary, SE India. Mar. Pollut. Bull. 2008, 56, 2043– 2051, DOI: 10.1016/j.marpolbul.2008.08.005

27 Sierra, A.; Jiménez-López, D.; Ortega, T.; Ponce, R.; Bellanco, M. J.; Sánchez-Leal, R.; Gómez-Parra, A.; Forja, J. Spatial and seasonal variability of CH4 in the eastern Gulf of Cadiz (SW Iberian Peninsula). Sci. Total Environ. 2017, 590–591, 695– 707, DOI: 10.1016/j.scitotenv.2017.03.030

28 Yang, P.; Yang, H.; Lai, D. Y. F.; Guo, Q.; Zhang, Y.; Tong, C.; Xu, C.; Li, X. Large contribution of non-aquaculture period fluxes to the annual N2O emissions from aquaculture ponds in Southeast China. J. Hydrol 2020, 582, 124550, DOI: 10.1016/j.jhydrol.2020.124550

29 Marescaux, A.; Thieu, V.; Garnier, J. Carbon dioxide, methane and nitrous oxide emissions from the human-impacted Seine watershed in France. Sci. Total Environ. 2018, 643, 247– 259, DOI: 10.1016/j.scitotenv.2018.06.151

30 Campeau, A.; Del Giorgio, P. A. Patterns in CH4 and CO2 concentrations across boreal rivers: Major drivers and implications for fluvial greenhouse emissions under climate change scenarios. Glob Chang Biol 2014, 20, 1075– 1088, DOI: 10.1111/gcb.12479

31 Xiao, Q.; Zhang, M.; Hu, Z.; Gao, Y.; Hu, C.; Liu, C.; Liu, S.; Zhang, Z.; Zhao, J.; Xiao, W.; Lee, X. Spatial variations of methane emission in a large shallow eutrophic lake in

subtropical climate. J. Geophys. Res.: Biogeosci. 2017, 122, 1597– 1614, DOI: 10.1002/2017jg003805

32 Yamamoto, S.; Alcauskas, J. B.; Crozier, T. E. Solubility of methane in distilled water and seawater. J. Chem. Eng. Data 1976, 21, 78– 80, DOI: 10.1021/je60068a029

33 Koné, Y. J. M.; Abril, G.; Delille, B.; Borges, A. V. Seasonal variability of methane in the rivers and lagoons of Ivory Coast (West Africa). Biogeochemistry 2010, 100, 21– 37, DOI: 10.1007/s10533-009-9402-0

34 Xiao, Q.; Hu, Z.; Fu, C.; Bian, H.; Lee, X.; Chen, S.; Shang, D. Surface nitrous oxide concentrations and fluxes from water bodies of the agricultural watershed in Eastern China. Environ. Pollut. 2019, 251, 185– 192, DOI: 10.1016/j.envpol.2019.04.076

35 Cole, J. J.; Caraco, N. F. Atmospheric exchange of carbon dioxide in a low-wind oligotrophic lake measured by the addition of SF6. Limnol. Oceanogr. 1998, 43, 647– 656, DOI: 10.4319/lo.1998.43.4.0647

36 Wanninkhof, R. Relationship between wind speed and gas exchange over the ocean. J. Geophys. Res. 1992, 97, 7373– 7382, DOI: 10.1029/92jc00188

37 Sibgh, S.; Bhatti, T. S.; Kothari, D. P. Wind power estimation using artificial neural network. J. Energy Eng. 2007, 133, 46– 52, DOI: 10.1061/(ASCE)0733-9402(2007)133:1(46)

38 da Silva, M. G.; Packer, A. P.; Sampaio, F. G.; Marani, L.; Mariano, E. V. C.; Pazianotto, R. A. A.; Ferreira, W. J.; Alvalá, P. C. Impact of intensive fish farming on methane emission in a tropical hydropower reservoir. Climatic Change 2019, 150, 195– 210

39 Beaulieu, J. J.; McManus, M. G.; Nietch, C. T. Estimates of reservoir methane emissions based on a spatially balanced probabilistic-survey. Limnol. Oceanogr. 2016, 61, S21– S40, DOI: 10.1002/lno.10284

40 Paranaíba, J. R.; Barros, N.; Mendonça, R.; Linkhorst, A.; Isidorova, A.; Roland, F.; Almeida, R. M.; Sobek, S. Spatially resolved measurements of CO2 and CH4 concentration and gas-exchange velocity highly influence carbonemission estimates of reservoirs. Environ. Sci. Technol. 2018, 52, 607– 615, DOI: 10.1021/acs.est.7b05138

41 Yang, L.; Lu, F.; Wang, X.; Duan, X.; Song, W.; Sun, B.; Zhang, Q.; Zhou, Y. Spatial and seasonal variability of diffusive methane emissions from the Three Gorges Reservoir. J. Geophys. Res.: Biogeosci. 2013, 118, 471– 481, DOI: 10.1002/jgrg.20049

42 Zheng, H.; Zhao, X.; Zhao, T.; Chen, F.; Xu, W.; Duan, X.; Wang, X.; Ouyang, Z. Spatial–temporal variations of methane emissions from the Ertan hydroelectric reservoir in southwest China. Hydrol. Process. 2011, 25, 1391– 1396, DOI: 10.1002/hyp.7903

43 Bevelhimer, M. S.; Stewart, A. J.; Fortner, A. M.; Phillips, J. R.; Mosher, J. J. CO2 is dominant greenhouse gas emitted from six hydropower reservoirs in southeastern United States during peak summer emissions. Water 2016, 8, 1– 14, DOI: 10.3390/w8010015

44 Li, S.; Bush, R. T.; Santos, I. R.; Zhang, Q.; Song, K.; Mao, R.; Wen, Z.; Lu, X. X. Large greenhouse gases emissions from China's lakes and reservoirs. Water Res. 2018, 147, 13– 24, DOI: 10.1016/j.watres.2018.09.053

45 Linkhorst, A.; Hiller, C.; DelSontro, T.; Azevedo, G. M.; Barros, N.; Mendonça, R.; Sobek, S. Comparing methane ebullition variability across space and time in a Brazilian reservoir. Limnol. Oceanogr. 2020, 69, 1623– 1634, DOI: 10.1002/lno.11410

46 Natchimuthu, S.; Sundgren, I.; Gålfalk, M.; Klemedtsson, L.; Crill, P.; Danielsson, Å.; Bastviken, D. Spatio-temporal variability of lake CH4 fluxes and its influence on annual whole lake emission estimates. Limnol. Oceanogr. 2016, 61, S13– S26, DOI: 10.1002/lno.10222

47 Bastviken, D.; Cole, J. J.; Pace, M. L.; Van de Bogert, M. C. Fates of methane from different lake habitats: connecting whole-lake budgets and CH4 emissions. J. Geophys. Res. 2008, 113, a, DOI: 10.1029/2007jg000608

48 Grinham, A.; Dunbabin, M.; Gale, D.; Udy, J. Quantification of ebullitive and diffusive methane release to atmosphere from a water storage. Atmos. Environ. 2011, 45, 7166– 7173, DOI: 10.1016/j.atmosenv.2011.09.011

49 Liikanen, A.; Flöjt, L.; Martikainen, P. Gas dynamics in eutrophic lake sediments affected by oxygen, nitrate, and sulfate. J. Environ. Qual. 2002, 31, 338– 349, DOI: 10.2134/jeq2002.3380

50 Huttunen, J. T.; Alm, J.; Liikanen, A.; Juutinen, S.; Larmola, T.; Hammar, T.; Silvola, J.; Martikainen, P. J. Fluxes of methane, carbon dioxide and nitrous oxide in boreal lakes and potential anthropogenic effects on the aquatic greenhouse gas emissions. Chemosphere 2003, 52, 609– 621, DOI: 10.1016/s0045-6535(03)00243-1

51 Hu, B.; Wang, D.; Zhou, J.; Meng, W.; Li, C.; Sun, Z.; Guo, X.; Wang, Z. Greenhouse gases emission from the sewage draining rivers. Sci. Total Environ. 2018, 612, 1454– 1462, DOI: 10.1016/j.scitotenv.2017.08.055

52 Silvennoinen, H.; Liikanen, A.; Rintala, J.; Martikainen, P. J. Greenhouse gas fluxes from the eutrophic Temmesjoki River and its estuary in the Liminganlahti Bay (the Baltic Sea). Biogeochemistry 2008, 90, 193– 208, DOI: 10.1007/s10533-008-9244-1

53 Alshboul, Z.; Encinas-Fernández, J.; Hofmann, H.; Lorke, A. Export of dissolved methane and carbon dioxide with effluents from municipal wastewater treatment plants. Environ. Sci. Technol. 2016, 50, 5555– 5563, DOI: 10.1021/acs.est.5b04923

54 Bastviken, D.; Cole, J.; Pace, M.; Tranvik, L. Methane emissions from lakes: Dependence of lake characteristics, two regional assessments, and a global estimate. Global Biogeochem. Cycles 2004, 18. DOI: 10.1029/2004gb002238

55 Hofmann, H.; Federwisch, L.; Peeters, F. Wave induced release of methane: Littoral zones as a source of methane in lakes. Limnol. Oceanogr. 2010, 55, 1990– 2000, DOI: 10.4319/lo.2010.55.5.1990

56 Li, M.; Peng, C.; Zhu, Q.; Zhou, X.; Yang, G.; Song, X.; Zhang, K. The significant contribution of lake depth in regulating global lake diffusive methane emissions. Water Res. 2020, 172, 115465, DOI: 10.1016/j.watres.2020.115465

57 Schilder, J.; Bastviken, D.; van Hardenbroek, M.; Kankaala, P.; Rinta, P.; Stötter, T.; Heiri, O. Spatial heterogeneity and lake morphology affect diffusive greenhouse gas emission estimates of lakes. Geophys. Res. Lett. 2013, 40, 5752– 5756, DOI: 10.1002/2013gl057669

58 West, W. E.; Creamer, K. P.; Jones, S. E. Productivity and depth regulate lake contributions to atmospheric methane. Limnol. Oceanogr. 2016, 61, S51– S61, DOI: 10.1002/lno.10247

59 Grinham, A.; Dunbabin, M.; Albert, S. Importance of sediment organic matter to methane ebullition in a sub–tropical freshwater reservoir. Sci. Total Environ. 2018, 621, 1199– 1207, DOI: 10.1016/j.scitotenv.2017.10.108

60 Marani, L.; Alvalá, P. C. Methane emissions from lakes and floodplains in Pantanal, Brazil. Atmos. Environ. 2007, 41, 1627– 1633, DOI: 10.1016/j.atmosenv.2006.10.046

61 Bastviken, D.; Cole, J. J.; Pace, M. L.; Van de Bogert, M. C. Fates of methane from different lake habitats: Connecting whole–lake budgets and CH4 emissions. J. Geophys. Res. 2008, 113, a, DOI: 10.1029/2007jg000608

62 Sundh, I.; Bastviken, D.; Tranvik, L. J. Abundance, activity, and community structure of pelagic methane-oxidizing bacteria in temperate lakes. Appl. Environ. Microbiol. 2005, 71, 6746– 6752, DOI: 10.1128/aem.71.11.6746-6752.2005

63 Yang, P.; Lai, D. Y. F.; Yang, H.; Tong, C.; Lebel, L.; Huang, J.; Xu, J. Methane dynamics of aquaculture shrimp ponds in two subtropical estuaries, southeast China: Dissolved concentration, net sediment release, and water oxidation. J. Geophys. Res.: Biogeosci. 2019, 124, 1430– 1445, DOI: 10.1029/2018jg004794

64 Matoušå, A.; Osudar, R.; Šimek, K.; Bussmann, I. Methane distribution and methane oxidation in the water column of the Elbe estuary, Germany. Aquat. Sci. 2016, 79, 443– 458, DOI: 10.1007/s00027-016-0509-9

65 Schrier-Uijl, A. P.; Veraart, A. J.; Leffelaar, P. A.; Berendse, F.; Veenendaal, E. M. Release of CO2 and CH4 from lakes and drainage ditches in temperate wetlands. Biogeochemistry 2011, 102, 265– 279, DOI: 10.1007/s10533-010-9440-7

66 Harrison, J. A.; Deemer, B. R.; Birchfield, M. K.; O'Malley, M. T. Reservoir water-level drawdowns accelerate and amplify methane emission. Environ. Sci. Technol. 2017, 51, 1267– 1277, DOI: 10.1021/acs.est.6b03185

67 Gunkel, G. Hydropower—A green energy? Tropical reservoirs and greenhouse gas emissions. Clean: Soil, Air, Water 2009, 37, 726– 734, DOI: 10.1002/clen.200900062

Table 1. Physicochemical Variables of the Surface Water (20 cm Depth) at Two Reservoir Zones from the Wenwusha Reservoir During Each Sampling Campaign [a]

	Nov-2018		Mar-2019		Jun-2019	
environmental variables	southern district	northern district	southern district	northern sistrict	southern district	northern district
W_T (oC)	17.82 ± 0.12a	18.72 ± 0.03a	23.23 ± 0.26a	22.99 ± 0.17a	29.52 ± 0.19a	29.07 ± 0.06a
pH value	10.69 ± 0.04a	10.70 ± 0.01a	8.94 ± 0.05a	8.35 ± 0.11a	6.13 ± 0.15a	7.51 ± 0.02b
EC (mS cm^{-1})	6.28 ± 0.10a	2.41 ± 0.08b	2.98 ± 0.08a	2.33 ± 0.08b	0.90 ± 0.03a	0.61 ± 0.01b
salinity	2.97 ± 0.05a	1.06 ± 0.02b	1.46 ± 0.03a	1.13 ± 0.03b	0.58 ± 0.01a	0.33 ± 0.01b
DO (mg L^{-1})	6.90 ± 0.28a	3.87 ± 0.08b	12.96 ± 0.34a	9.56 ± 0.56b	5.93 ± 0.20a	3.64 ± 0.11b
$N-NO_3^-$ (mg L^{-1})	1.05 ± 0.10a	1.83 ± 0.08b	0.57 ± 0.08a	1.79 ± 0.04b	0.80 ± 0.03a	1.08 ± 0.05b
$N-NH_4^+$ (mg L^{-1})	0.42 ± 0.05b	0.72 ± 0.04a	0.17 ± 0.01a	0.37 ± 0.04b	0.50 ± 0.03a	0.89 ± 0.03a
TOC (mg L^{-1})	16.23 ± 0.61a	22.43 ± 0.53b	18.08 ± 0.60a	22.63 ± 0.73b	16.75 ± 0.0.72a	21.92 ± 0.55b

[a] W_T, EC, DO, and TOC represent the water temperature, conductivity, dissolved oxygen, and total dissolved carbon, respectively. Lowercase letters within the same row indicate significant differences at $p < 0.05$ level between two reservoir zones during each sampling campaign.

Table 2. Spearman Correlation Coefficients between Diffusive CH_4 fluxes and Environmental Variables at the Wenwusha Reservoir *a*

	diffusive CH_4 fluxes			
environmental variables	Nov-2018	Mar-2019	Jun-2019	all data
Meteorological Factors				
air temperature	0.445**	NS	NS	0.191**
wind speed	NS	NS	NS	NS
atmospheric pressure	−0.249*	NS	NS	NS
Physical-Chemical Variables of Water				
water temperature	0.523**	NS	NS	0.135*
pH value	NS	−0.472**	0.364*	−0.114*
conductivity (EC)	−0.338**	−0.260**	−0.234*	−0.313**
salinity	−0.469**	−0.263**	NS	−0.353**
dissolved oxygen (DO)	−0.736**	−0.554**	−0.339**	−0.501**
$N-NO_3^-$	NS	NS	NS	NS
$N-NH_4^+$	0.472**	0.230*	0.226*	0.369**
total dissolved carbon (TOC)	0.790**	0.735**	0.632**	0.711**

[a] n = 103 for environmental variables and CH_4 fluxes of the reservoir during each sampling campaign. The symbols * and ** denote significant correlations at $p < 0.05$ and $p < 0.01$, respectively. NS means “not significant”. Bold numbers denote statistically significant correlation coefficients.

Table 3. Mean and Total Diffusive CH_4 Fluxes for Different Upscaling Scenarios *a*

scenario	time	data set	mean flux (μg m^{-2} h^{-1})	total flux (Gg CH_4 yr^{-1})
*	all sampling seasons	all sampling sites	257.2	0.012
I	all sampling seasons	47 sampling sites of the SRZ	161.0	0.007
	all sampling seasons	56 sampling sites of the NRZ	337.9	0.016
II	all sampling seasons	64 sampling sites from the nonsewage loading areas	98.6	0.004
	all sampling seasons	39 sampling sites from the sewage loading areas	629.9	0.029
III	all sampling seasons	42 sampling sites from the shallow areas	476.5	0.022
	all sampling seasons	61 sampling sites from the deep areas	106.7	0.005
IV	all sampling seasons	6 sampling sites from the transect 2#	48.9	0.002
	all sampling seasons	3 sampling sites from the transect 12#	2047.8	0.095

a The total fluxes were calculated from the products of the mean flux and total reservoir area (5.2 km^2). The asterisk represents our best flux estimate derived from spatially averaged flux from all 103 sites across all the sampling campaigns.

Table 4. Range of Dissolved CH_4 Concentrations (nmol L^{-1}), Saturations (%), and Diffusive Fluxes (μmol m^{-2} h^{-1}) in Reservoirs [a]

site	date	CH_4 concentration	CH_4 saturation	diffusive fluxes	references
Fujian Province, China	Nov 2018, Mar and Jun 2019	30−27,300 (403)	42−42,460 (634)	−4.5−724.0 (16.1)	this study
sixteen small reservoirs, Chongqing, China	Sep 2014 to Jun 2015	60−1880 (340)	2684−83,668 (---)	7.5−203.8 (39.2)	9
three subtropical reservoirs, Queensland, Australia	Aug 2011 to May 2012	36−11,836 (---)	1350−523,987 (---)	5.9−53.4 (25.8)	8
Furnas hydroelectrical reservoir, Brazil	Aug 2013 to Nov 2014	6−969 (163)		9.9−29.9 (15.3)	38
Eguzon reservoir, France	Jan to Dec 2011	10−30,500 (---)		0.0−629.2 (62.5)	20
Three Gorges reservoir, China	Jan to Dec 2010			1.5−117.3 (20.6)	41
Chapéu D'Uvas, Brazil	Sep 2015			1.7−666.7 (66.7)	40
Curuá-Una, Brazil	Mar 2016			3.8−287.5 (25.0)	40
Furnas, Brazil	Jun and Jul 2015			0.04−895.8 (104.2)	40
Ertan hydroelectric reservoir, China	May 2008 to April 2009			------- (116.7)	42
Lake Kariba, Zambia/Zimbabwe	Jul 2007, May 2008, Feb and Jun 2009	100−2000 (---)	3731−74,627		4
Harsha, USA	Oct 2012 to Nov 2012	10−15630 (---)		304.7−2236.9 (608.3)	22
Harsha, USA	Aug and Sep 2014	140−3120 (735)		4.4−386.3 (37.5)	39
Allatoona, Douglas, Fontana, Guntersville, Hartwell, Watts Bar, USA	Aug and Sep 2012			15.8−487.5 (---)	43
temperate reservoirs				------- (30.3)	11
temperate reservoirs				------- (38.5)	14
China's reservoirs				------- (26.8)	56
global reservoirs				------- (312.5)	12

[a] Notes: the numbers within parentheses refer to average value.

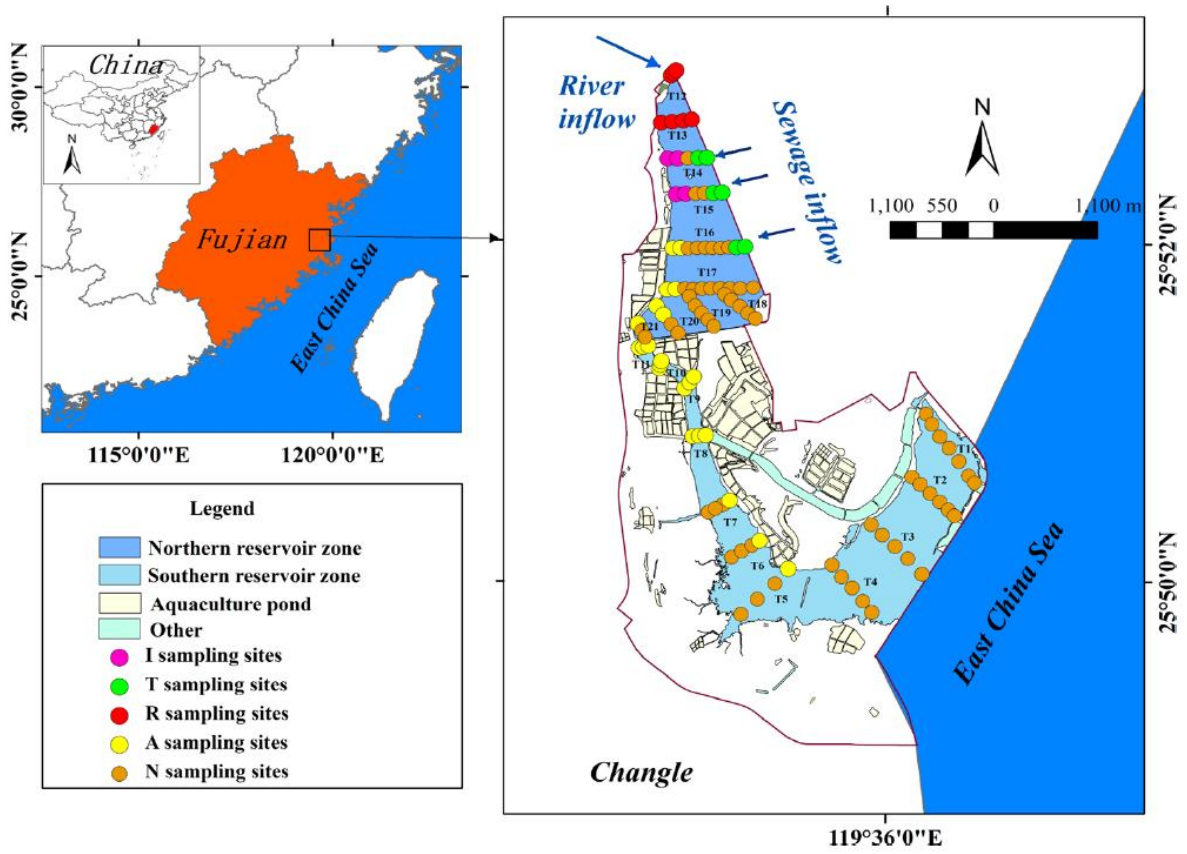

Figure 1. Geographical location of the Wenwusha Reservoir and the sampling sites in Fujian, Southeast China. SRZ and NRZ represent the southern and northern reservoir zones, respectively. A total of 21 transects were selected for sampling across the whole reservoir, with 11 transects in SRZ (T1–T11), and 10 in NRZ (T12–T21). I, T, R, A, and N represent industrial effluent, town sewage, river input, aquaculture sewage, and nonsewage discharge points, respectively.

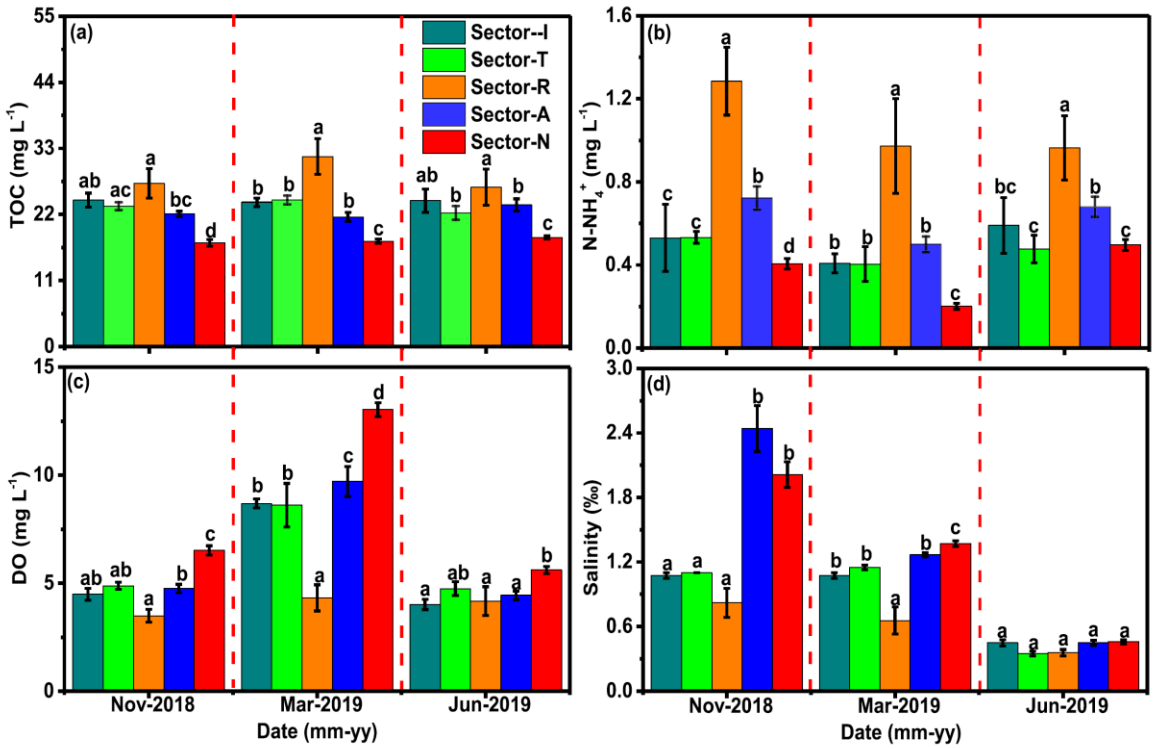

Figure 2. Variations in (a) surface water TOC, (b) N–NH_4^+, (c) DO, and (d) salinity at the different sewage loading areas across the whole Wenwusha Reservoir during each sampling campaign. The various lowercase letters on the bars indicate significant differences at the $p < 0.05$ level because of the varying sewage loading areas during each sampling campaign. Sector-I, Sector-T, Sector-R, Sector-A, and Sector-N represent the industrial effluents loading sectors ($n = 4$ sampling sties), town sewage loading zone ($n = 6$ sampling sties), river input zone ($n = 7$ sampling sties), aquaculture sewage loading zone ($n = 22$ sampling sties), and nonwastewater loading zone ($n = 64$ sampling sties), respectively. Bars represent mean ± SE.

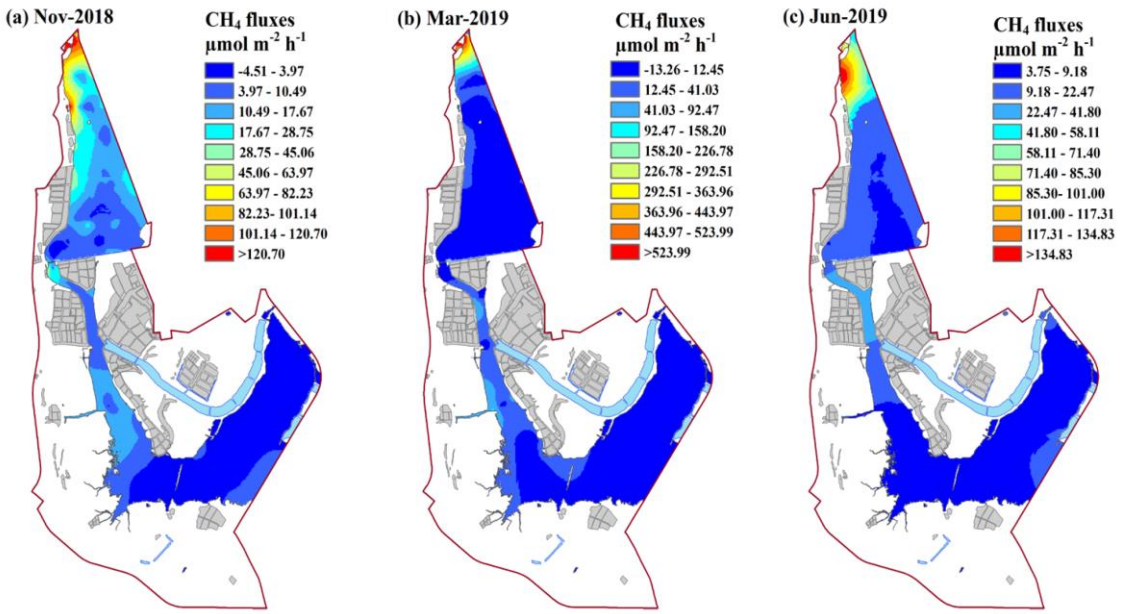

Figure 3. Spatial variations in the CH_4 diffusion flux across the water–atmosphere interface from the Wenwusha Reservoir in November 2018 (a), March 2019 (b), and June 2019 (c).

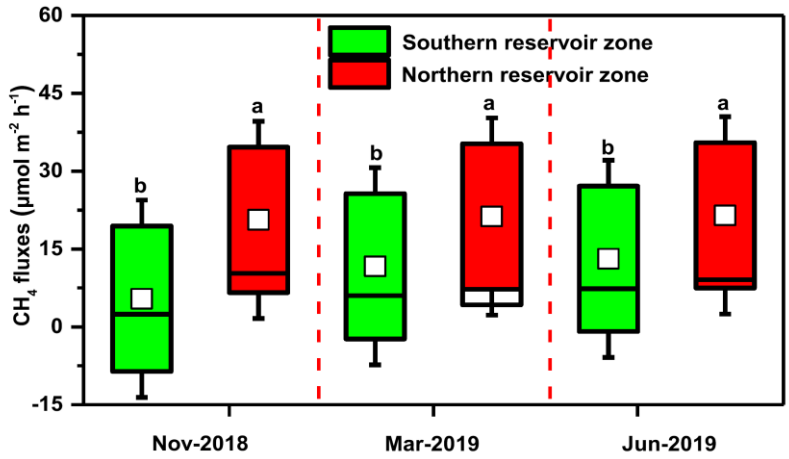

Figure 4. Variations in diffusive CH_4 flux at the different reservoir zones from the Wenwusha Reservoir during each sampling campaign. Different lowercase letters above the bars indicate significant differences at the $p < 0.05$ level between the SRZ ($n = 47$) and NRZ ($n = 56$).

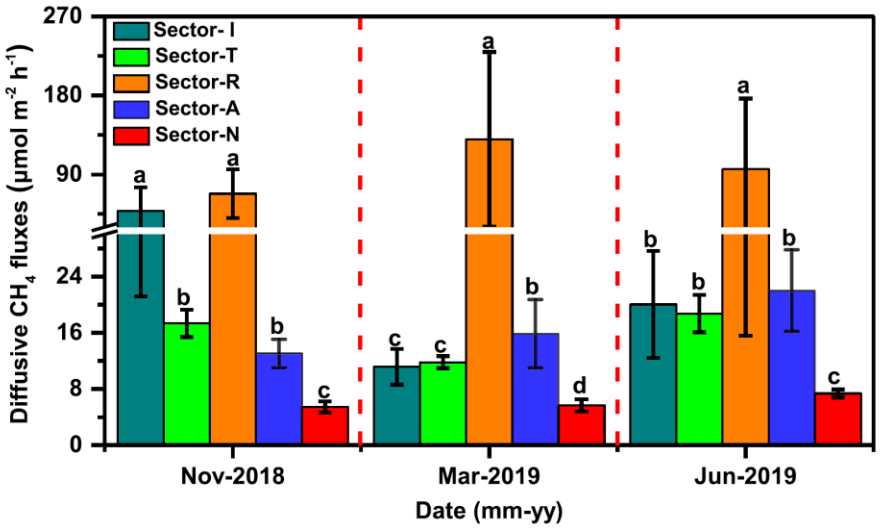

Figure 5. Variations in diffusive CH_4 flux among different sewage loading areas across the whole Wenwusha Reservoir during each sampling campaign. The various lowercase letters on the bars indicate significant differences at the $p < 0.05$ level because of the varying sewage loading areas during each sampling campaign. Sector-I, Sector-T, Sector-R, Sector-A, and Sector-N represent the industrial effluents loading sectors (n = 4 sampling sties), town sewage loading zone (n = 6 sampling sties), river input zone (n = 7 sampling sties), aquaculture sewage loading zone (n = 22 sampling sties), and nonwastewater loading zone (n = 64 sampling sties), respectively. Bars represent mean ± SE. Bars represent mean ± SE.

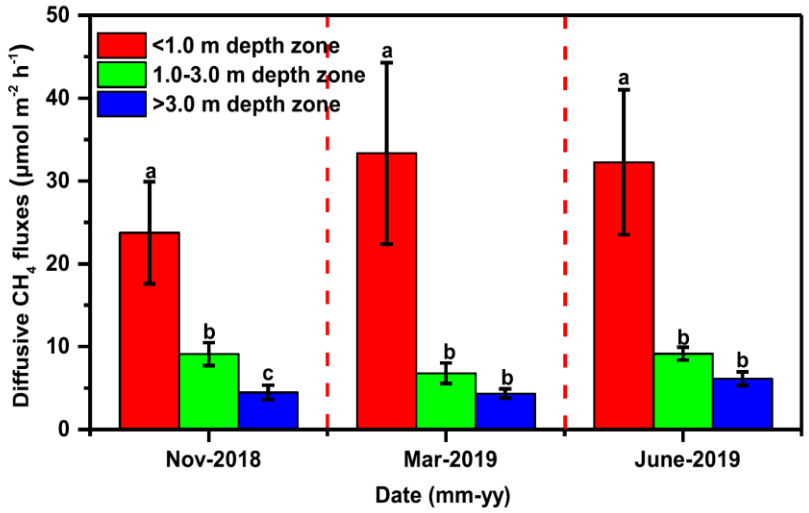

Figure 6. Variations in diffusive CH_4 flux at the different water depth zones across the whole Wenwusha Reservoir during each sampling campaign. Different lowercase letters above the bars indicate significant differences at the $p < 0.05$ level between the different water depth zones. n = 42, 30, and 31 for < 1 m depth zone, 1–3 m zone, and >3 m zone, respectively.

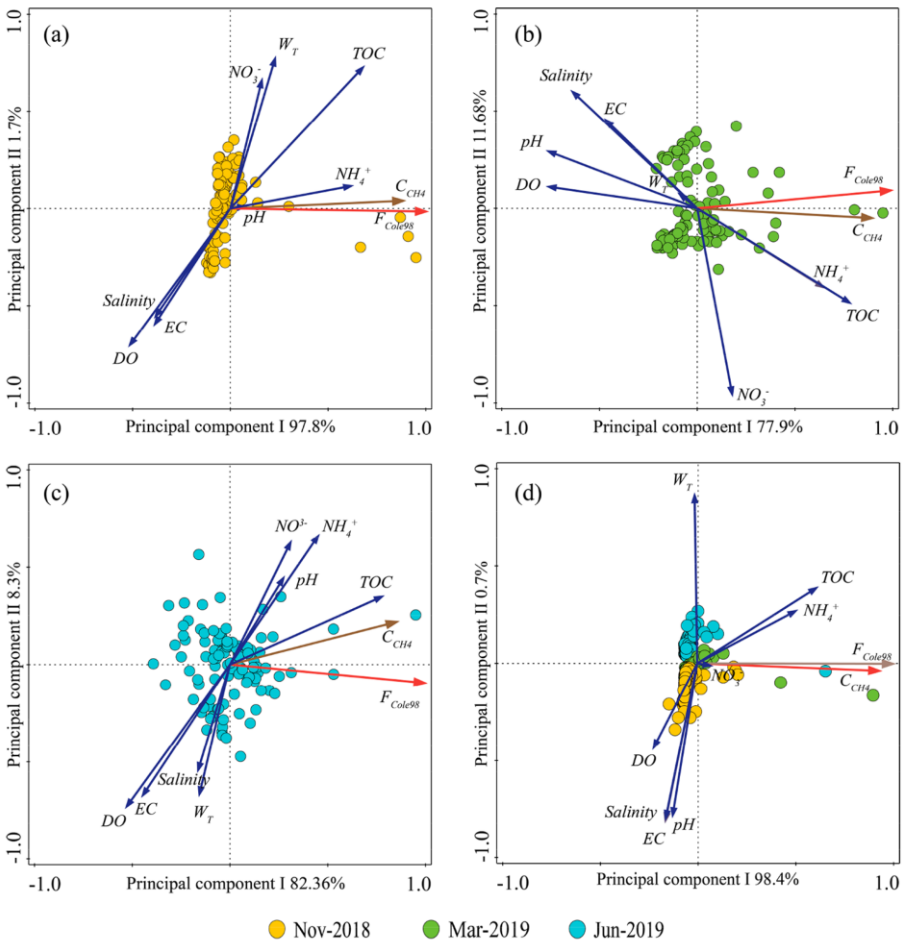

Figure 7. PCA biplots of the CH_4 concentration (or CH_4 fluxes) and surface water characteristics of the Wenwusha Reservoir, showing the loadings of ancillary water quality parameters (arrows) and the scores of observations in three sampling campaigns [Nov-2018 (a), Mar-2019 (b), and Jun-2019 (c)] and in all sampling campaign all together (d). W_T, DO, EC, C_{CH4}, and F_{Cole98} represent the water temperature, dissolved oxygen, conductivity, dissolved CH_4 concentration, and CH_4 diffusive flux, respectively.

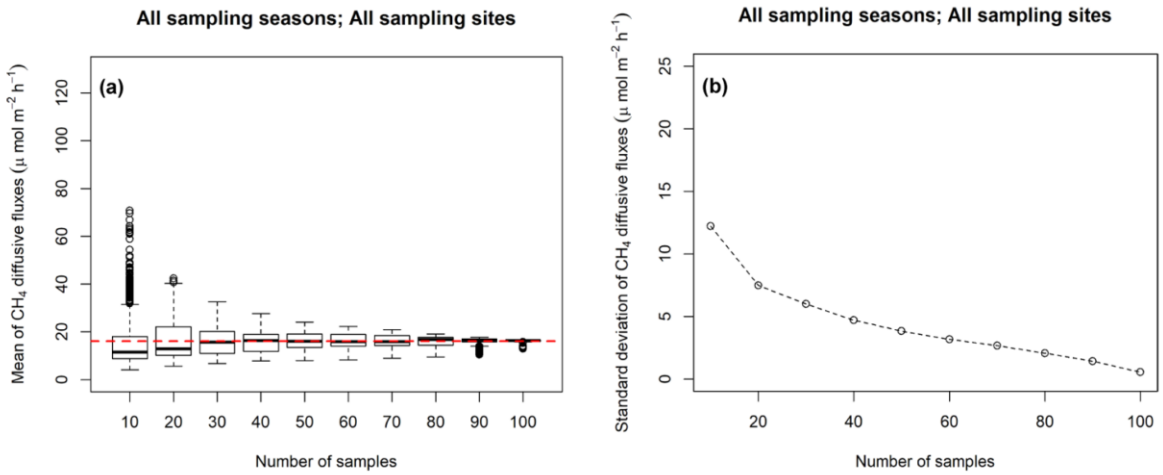

Figure 8. (a) Box and whisker plots and (b) standard deviation of estimated whole-reservoir CH_4 diffusive fluxes as a function of the number of sampling sites selected from a total of 103 sites without replacements based on 1000 simulations. The margins of the boxes represent the upper and lower quartiles, and the line in the box is the median value. The whiskers represent the extreme values that fall within 1.5 times the interquartile range from the box. The circles present the extreme values that are over 1.5 times the interquartile range. The red line represents the overall mean CH_4 flux based on the data from all 103 sites.